Int. J. Multiphase Flow Vol. 19, No. 1, pp. 99–113, 1993
Printed in Great Britain

0301-9322/93 $6.00 + 0.00
Pergamon Press Ltd

BUBBLE SIZE AND ENTRANCE LENGTH EFFECTS ON VOID DEVELOPMENT IN A VERTICAL CHANNEL

T. J. LIU

Thermohydraulic Laboratory, Institute of Nuclear Energy Research, P.O. Box 3–3, Lung-Tan 32500, Taiwan, R.O.C.

(Received 2 June 1991; in revised form 10 March 1992)

Abstract—The effects of bubble size and entrance length on the void distribution in a vertical upward cocurrent air–water two-phase flow were studied systematically based on the measurements of a dual-sensor resistivity probe. The experiments were carried out under various fixed gas and liquid fluxes, with only the bubble size being changed at the flow entrance. Profiles of void fraction, bubble frequency, bubble velocity and bubble size were measured along the test section diameter at four axial positions with an entrance length (L)-to-internal diameter (D) ratio of 30, 60, 90 and 120, respectively, to study the void development phenomena. The test conditions cover both the wall and core peaking void distributions of two-phase bubbly flow. It is found that the bubble lateral migration and flow regime transition are very sensitive to the variation in bubble size and the bubble coalescence effect during the development of bubbly flow. Hence, existing models, which are to be valid over a wide range of conditions, should include the effect of bubble size.

Key Words: void fraction, bubble size, bubbly flow, flow regime, local measurement, resistivity probe, two-phase flow structural development

1. INTRODUCTION

The effect of bubble size on the lateral void fraction distribution is essential in understanding the detailed internal bubbly flow structure, and is directly related to mass, momentum and energy exchange from one phase to the other. The flow structure along a vertical channel resulting from the expansion of the gas phase associated with the frictional pressure gradient causes a continual lateral void fraction development. Thus, measurements of lateral void fraction should be accompanied by measurements of other structural parameters along the axial distance to gain insight into the flow structure development. The pioneering contributions of Serizawa *et al.* (1975) and Herringe & Davis (1976) in this area, using a resistivity probe to measure void fraction, bubble size and structure developing parameters, provided the impetus for further studies. Along with further experimental study of two-phase upward cocurrent bubbly flow in a circular pipe, two typical void profiles have been widely reported, namely coring (Jones & Zuber 1978; Van Der Welle 1985) and sliding (Michiyoshi & Serizawa 1986; Wang *et al.* 1987; Liu & Bankoff 1993) bubble flows and their combination. These peculiar profile configurations have been found to be greatly dependent on the initial condition (bubble size, generation method and mixing condition), the flow condition (flow rates and physical properties of different phases) and the test section condition (geometry and wall surface). On the other hand, the same local void fraction may be due to either a large number of small bubbles or a small number of large bubbles—although these two cases differ in both local flow turbulent structure and in interfacial contact area. This implies that even performing the experiment with a similar test section geometry under the same gas and liquid fluxes, the flow structure can be quite different.

Recently, the importance of bubble size effects have been stressed by Serizawa & Kataoka (1987; Kataoka & Serizawa 1990), Zun (1988), Lahey (1990) and others as a key parameter in flow modeling. Generally, the existing models are based on the following three major mechanisms: (1) the lift and/or Magnus effects associated with the mean flow (Wallis & Richter 1973; Zun 1980, 1988; Avdeev 1984); (2) the effect of liquid turbulence (Subbotin 1971; Rouhani 1976; Lahey 1988); and (3) the effect of bubble deformation (Lackme 1967; Kobayashi *et al.* 1970; Sekoguchi *et al.* 1979; Kariyasaki 1985). These proposed mechanisms shed light on the behavior of bubble movement; however, the detailed effect of bubble size is still not clear due to the complex interactions among the bubbles, liquid and channel wall. Therefore, it is found that the prediction of the void fraction distribution in this flow is constrained by insufficient experimental data on the

effect of different parameters. Among these, the bubble size effect is one of the most important problems to be solved experimentally.

Most of the previous experimental information concerning the effect of bubble size has been obtained using different bubble generators (e.g. Herringe & Davis 1976; Avdeev 1984; Matsui 1988; Takamasa 1989). However, under fixed gas and liquid flow rates, the bubble size from these conventional-type bubble generators cannot be controlled by the experimenter; this limitation makes it very hard to elucidate the parametric effect. In addition, the use of different bubble generators has inevitably mixed the effect of the inlet flow condition with the effect of bubble size. To understand the bubble size effect specifically, it is necessary to perform a series of experiments under various fixed gas and liquid flow rates conditions using a single bubble generator to create different sizes of bubbles at the inlet. At present, only one such study is known (Serizawa *et al.* 1988, 1991). Serizawa used a specially designed bubble generator to change the bubble size under the same two phase flow rates, in which the bubble size was carefully controlled and identified.

The objective of the present study is to extend the author's previous work (Liu & Bankoff 1993), using a new bubble generator which is a modification of Serizawa's design, with particular emphasis on the effects of the bubble size and axial length from the entrance on the behavior of structural development under well-controlled inlet bubble size flow conditions. The influences of system parameters, such as the mean flow velocity of the two phases are also examined.

2. TEST FACILITY AND PROCEDURE

Experiments were performed in an 8 m long, vertical smooth Lexan tube, with i.d. = 57.2 mm. The two-phase flow was realized by separately supplied and controlled flow rates of filtered air and

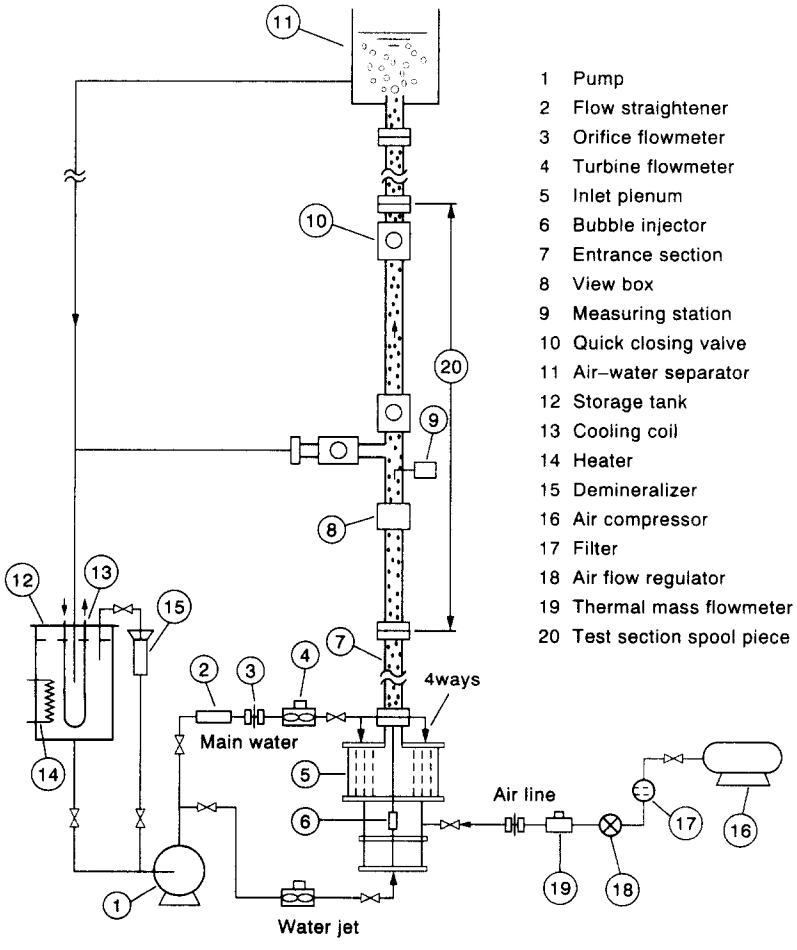

Figure 1. Schematic diagram of the experimental facility.

water through a specially designed bubble generator which were then mixed in the test section. The overall loop schematic is illustrated in figure 1. Details of the experimental facility are documented in Liu (1990).

The novel bubble generator design, to change the bubble size at the test section entrance under the same combination of gas and liquid volumetric fluxes was first presented by Serizawa *et al.* (1988). In principle, the compressed air in the air housing was injected through a porous cylinder wall into the water and was sheared away by the high-speed water jet. The bubble size was thus controlled by setting the water jet flow rate at an appropriate value.

In this study, a bubble generator similar to Serizawa's design but with slight modifications, as shown in figure 2, provides a stable two-phase inlet flow condition. To stabilize the air flow in the air chamber, a layer of fine mesh was installed around the porous cylinder with a nominal porosity of 7 μm. Before shearing the bubbles, the water jet flowed through two fine mesh screens installed in the water chamber to stabilize the jet flow. The liquid jet flow, J_j, accompanied by the generated bubbles thus entered the test section and mixed with the main liquid stream. Here, J_j is defined as the volumetric flux of water flow through the bubble injector with i.d. = 9.7 mm. To stabilize the resultant inlet test-section flow field and to eliminate secondary effects, the mixing quality of

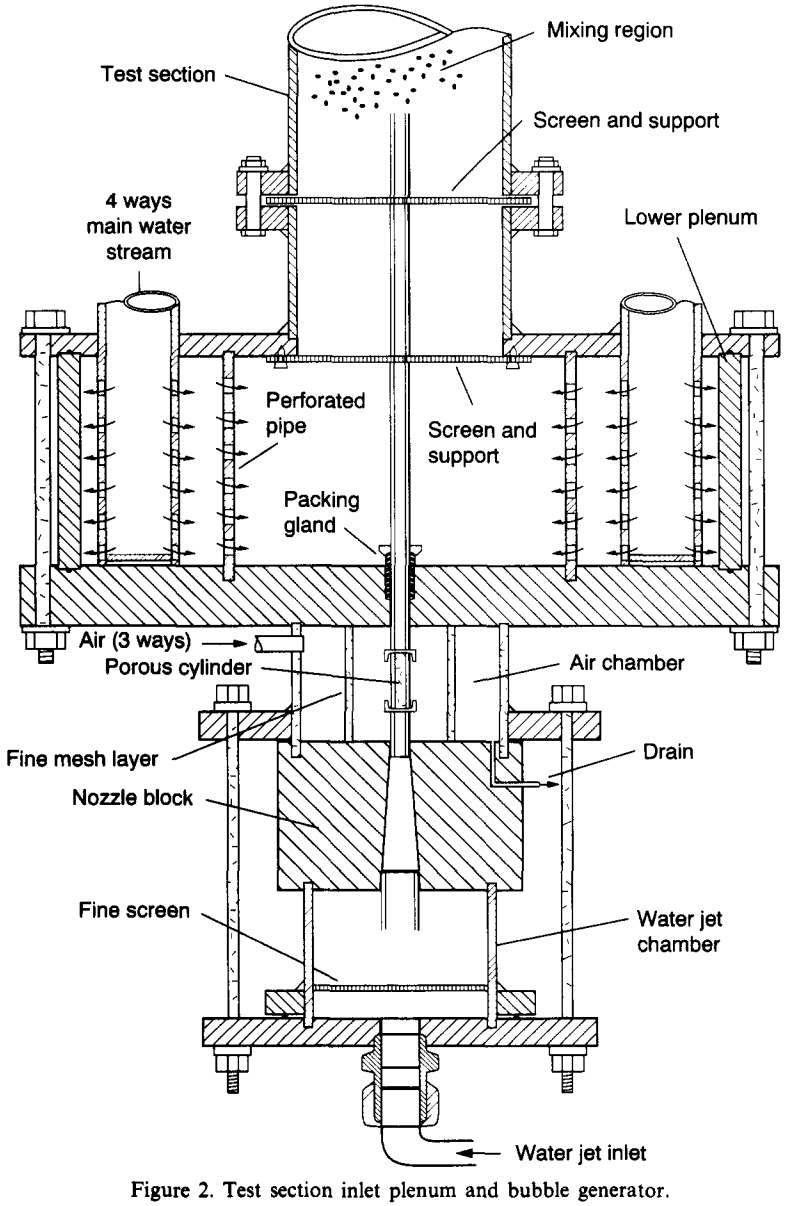

Figure 2. Test section inlet plenum and bubble generator.

the main liquid stream with the two-phase jet is significant. Here, the main liquid stream was first driven through four identical perforated sections arranged symmetrically in the inlet plenum and well-mixed therein by passing through a central perforated tube, as shown in figure 2. Finally, the main water stream flowed upward through a series of fine mesh screens at the entrance of the test section and then mixed uniformly with the two-phase jet. The total liquid volumetric flow rate into the test section was thus the sum of the liquid jet and main flows, which were controlled separately. Thus, a wide range of initial bubble size from <1 to 20 mm can be generated.

A miniature L-shaped dual-needle electrical resistivity probe was designed, which is suitable for use in high-speed, condensed small bubble two-phase flow. Details of the probe design are given in Liu (1991). Each sensor was driven by a voltage-sensitive circuit consisting of a 1.5 V battery and a 100 kΩ potentiometer connected in series with the probe grounded. The voltage level across the probe during a closed circuit (liquid signal) was approx. 0.3–0.4 V and that for an open circuit (gas signal) was approx. 0.5–0.8 V, depending on the flow conditions and bubble sizes. This low voltage effectively reduced fluid electrolysis on the sensor.

Prior to the formal test, the gas flow rates were corrected *in situ* by an interactive software to compensate for the deviation between the actual flow condition at the measuring stations and the calibration condition. In a typical run, the flow temperature (25°C at the measuring position) and the water and air flow rates (J_L and J_G) in the test section were held constant, while adjusting the flow rate of the water jet (J_j) through the bubble generator to change the bubble size. During the course of the experiment, the analog output signals of the two sensors were monitored by an oscilloscope and sampled by a high-speed data acquisition system (TSI IFA-200). A sampling rate of 10–20 kHz/channel was used to ensure sufficient resolution in analyzing the high-speed, small bubble, two-phase conditions. At each local measuring point, a sampling period of 10–30 s was used to detect a sufficient number of bubbles. All the information digitized by the computer was stored for further processing.

3. SIGNAL PROCESSING

A software of adjustable level and slope thresholds was employed in the phase discrimination stage to obtain the binary signal from the raw data. The transition between the gas and liquid phases was determined by comparing the instantaneous slope and magnitude of the probe voltage with the selected thresholds. The appropriate threshold could be selected in an iterative way so that the integrated local void fraction converged to the area-averaged void fraction $\langle \epsilon \rangle$. Thus, the local void fraction, $\epsilon(r)$, is determined by the fraction of totally digitized samples which is detected as gas, while the local bubble impact frequency, BF(r), is the number of counted bubbles averaged over the total sampling time. Previous studies (Liu 1989) have confirmed the reliability of this sampling technique.

The time-averaged local bubble velocity, $U_b(r)$, can be determined if the mean transport time, $\tau_0(r)$, of the bubble to pass through a fixed axial distance between the tips of the sensors, d, is known; such that, $U_b(r) = d/\tau_0(r)$. In this study, the cross-correlation function of the two sensor output signals was calculated to determine the most probable transport time, $\tau_0(r)$, at the clearly-defined peak of the correlogram. The local mean bubble size, $D_b(r)$, was determined from the measured bubble chord length histogram, $x(r)$, based on a statistical treatment of the bubble residence time. The method of Herringe & Davis (1976) was used to interpret the present data in terms of bubble size. Thus, the local mean bubble diameter can be determined by integration of the measured bubble chord length probability density function, $g(x)$, as

$$D_b(r) = 1.5 \int_0^\infty x \cdot g(x) \mathrm{d}x. \tag{1}$$

In order to check the accuracy of the locally-measured parameters, the integral of the product of the local bubble velocity and void fraction over the cross-section area, $\langle \epsilon \cdot U_b \rangle$, was compared with the gas superficial velocity, J_G, measured from the calibrated gas flowmeter. Ideally, these two values will be identical. After repeatability tests, the results indicated that the deviation of these two values is within 10% for more than 90% of the total 115 flow conditions investigated in this study. The largest deviation appeared to be due to the presence of large air slugs for some limited

flow conditions. Experiments were performed under the following conditions:

- J_L (m/s) = 0.5, 1.0, 2.0 and 3.0
- J_G (m/s) = 0.1, 0.2 and 0.4
- J_j (m/s) = 0–6.0
- L/D = 30, 60, 90 and 120
- r/R = 0–98% (15 local points)
- $\langle \epsilon \rangle$ = 0–25%

4. RESULTS AND DISCUSSION

Profiles of void fraction were measured along the test-section diameter at four axial positions, with L/D = 30, 60, 90 and 120 respectively, to study the void development in turbulent two-phase flow under well-controlled bubble size injection. Generally, the higher the liquid jet velocity, J_j, the smaller are the generated bubbles. However, the exact bubble number density, bubble size and their distribution strongly depend on the combination of the liquid and gas volumetric fluxes, J_L and J_G, and the axial distance from the injection point (or entrance length), L. All of these effects will contribute to the specific distribution of the void fraction. To understand the internal flow structure and to elucidate the mechanism of turbulent transfer in two-phase flows, the velocity profiles and the number and size of the bubbles were also measured simultaneously.

4.1. Two-phase mixing properties in the entrance region

As mentioned above, the bubble size can be changed and controlled at the flow entrance by using a special bubble generator to study the effects of bubble size on the development of the void distribution under various fixed gas and liquid fluxes. The two-phase flow is realized by mixing the coaxial two-phase jet with the upward surrounding main water stream at the inlet of the test section. It is essential that the mixing quality of the inlet conditions should be clearly assessed. Depending on the flow conditions, the small bubbles in the inverted-conical two-phase round jet injected from the inlet of the test section will travel a characteristic mixing length where the boundary of the jet is extended to the pipe wall. Generally, the higher the main liquid flow rate and/or the lower the gas flow rate and/or the higher the liquid jet flow rate (i.e. the smaller the bubble size), the larger is the mixing length—due to the high axial inertia force of the two-phase jet outweighing the lateral mixing effect. It is observed that the mixing length is $< 5D$ for all the flow conditions investigated.

In order to evaluate the performance of the bubble generator used in this study, the development of two-phase flow at the entrance region has been examined in detail by measuring the radial profiles of the local void fraction, bubble frequency, bubble velocity and bubble size along the test-section diameter from $r/R = -0.93$ to $+0.93$ at the different entrance lengths of L/D = 12, 20 and 30. Typical results are presented in figures 3(a,b) for the two different flow conditions. It can be seen from the figures that all the profiles of these four parameters are axially changing symmetrically during the course of flow development. At L/D = 12, most of the small bubbles were crowded at the center, resulting in a convex profile of the void fraction and bubble frequency distributions. With further development, bubbles gradually grow and are transported from the jet core into the wall. As a result, the peak height of the gas content increases with the distance from the injection point and the lower the gas content in the core. It should be noted that a relatively larger bubble size was measured near the wall. The observed maxima near the wall may be due to the highly concentrated bubbles having a greater probability of bubble coalescence. The elongated bubble in the flow direction caused by the large gradient of the shear stress near the wall may be another reason. The development of the bubble velocity maintains the parabolic profile, which did not present changes as significant as those in the void fraction and bubble frequency, but slightly increased as the bubble size increased with the distance from the injection point. This is due to the expansion of the gas phase associated with the frictional pressure gradient causing a continuous acceleration of the mixture. Consequently, a continual axial cylindrical symmetry flow development along the tube could be expected. All these experimental results reveal that the quality of the inlet condition is good enough to study the effect of bubble size on the two-phase flow structure development.

4.2. Flow regime development

Figure 4 presents a typical result based on the qualitative observations of flow regime development. The results indicate that different bubble sizes injected into the two fixed J_L and J_G

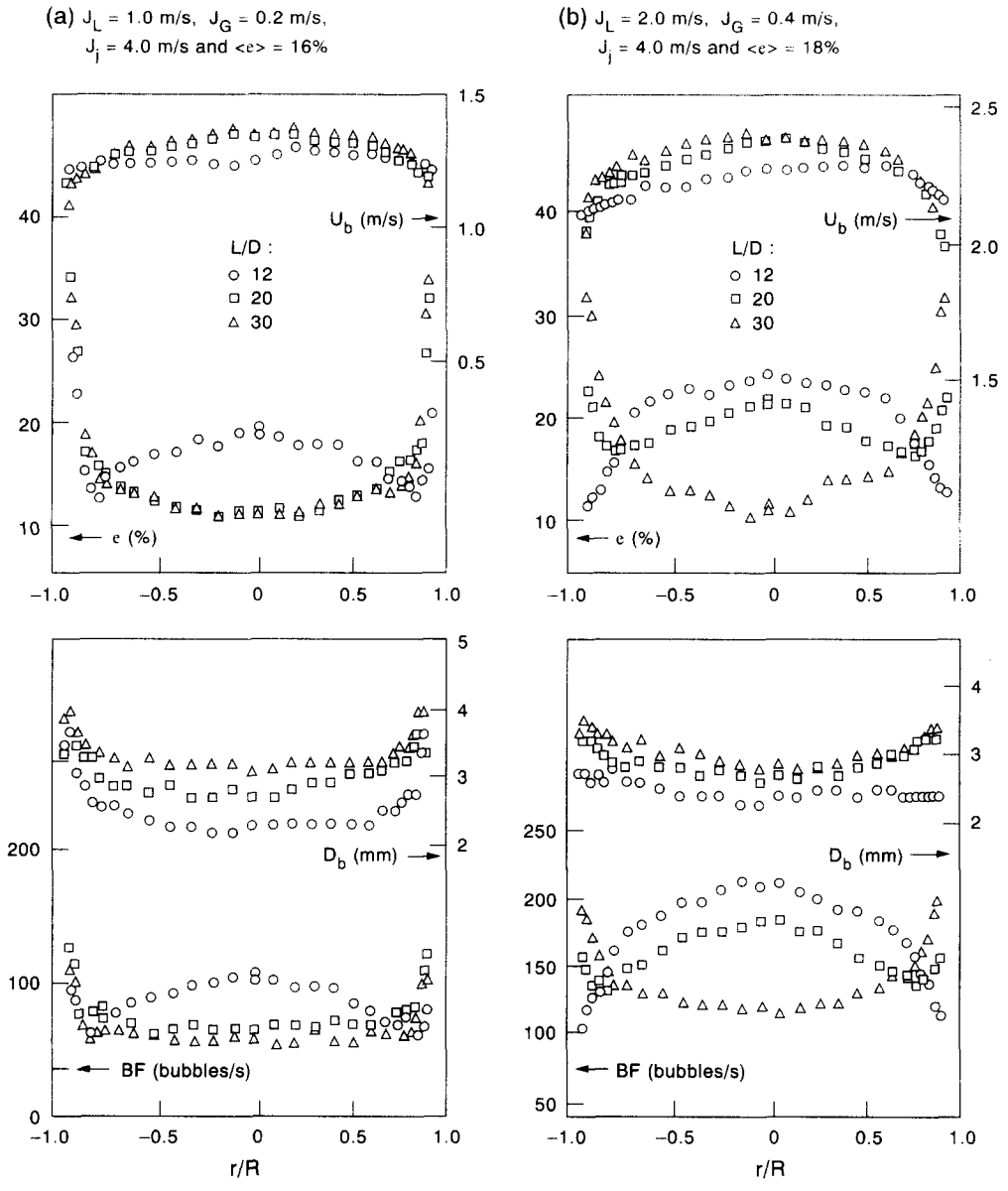

Figure 3. Two-phase mixing properties at the entrance region.

flow conditions show a drastic change in their flow patterns along the channel. Generally, the larger the bubble generated at the inlet, the faster the slug-like flow regime will be attained. In contrast, as the bubble size decreases to some extent, bubbly flow will appear. If the bubble size is reduced further, a stable bubbly flow will be developed along the whole length of the channel. This implies that the bubble size is the important parameter which affects the flow regime development. However, the existing published flow regime maps cannot reflect this result, as shown in figure 5. Performing the experiment for different bubble sizes could also be one of the reasons for the inconsistency between them. Moreover, the generally accepted criteria that bubbly flow will be maintained for a mean void fraction within 30% or other values is problematic without considering the bubble size.

4.3. Bubble size effect at a fixed entrance length

Figure 6(a) presents a typical result of void profile development under different bubble size conditions, which were controlled by adjusting the flow rate of the liquid jet, J_j, in the bubble generator, at $J_L = 1.0$ m/s, $J_G = 0.2$ m/s and $L/D = 60$. The corresponding bubble size, frequency

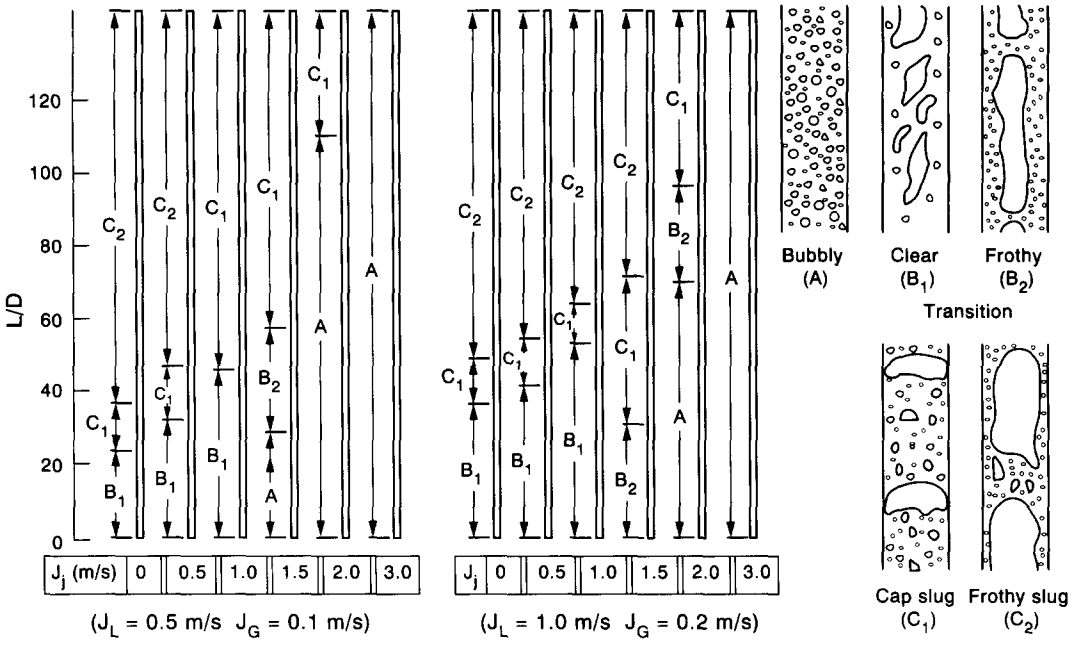

Figure 4. Flow regime development under different bubble size injections.

and velocity profiles are also shown in figures 6(b–d). From these figures, it should be noted that the size and number of bubbles generated are very sensitive to the value of J_j, while the void profile shows a strong dependence on the bubble size even under the fixed liquid and gas fluxes. The bubble velocity maintains the same parabolic profile which did not present as significant a change as void fraction, but slightly increased with bubble size. Generally, the smaller the bubbles generated, the more uniform are the bubble sizes distributed across the channel. Most of these small bubbles preferably migrate toward the tube wall resulting in a saddle-shaped bubble frequency profile, flatter in the core region. Therefore, the profiles of void fraction generally follow the same tendency as bubble frequency in this low J_L bubbly flow, as shown in figure 6(a). As the liquid jet decreases,

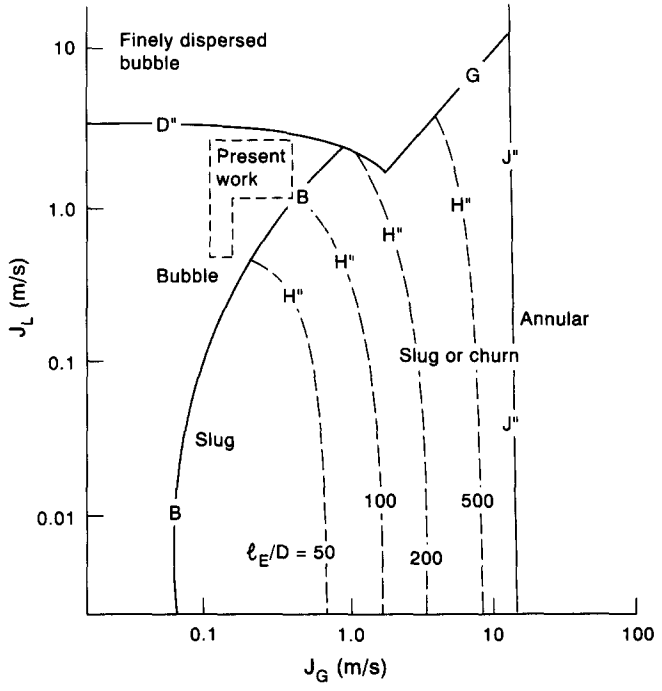

Figure 5. Flow regime map for vertical flow (Taitel *et al.* 1980).

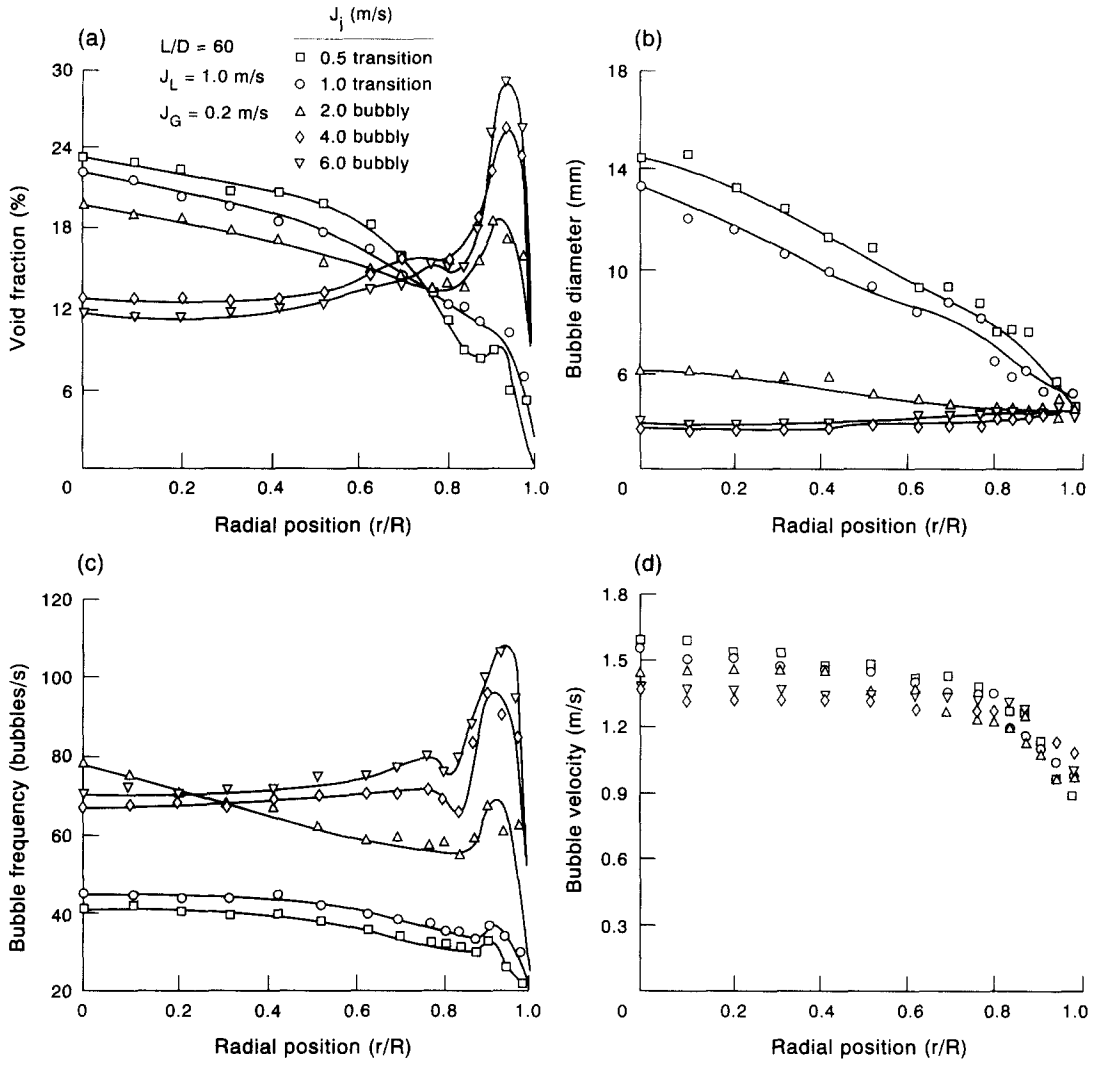

Figure 6. Bubble size effect on the (a) void fraction, (b) bubble size, (c) bubble frequency and (d) bubble velocity distributions.

the bubble size will be increased. This effect will lower the height of the void peak near the wall. As the nozzle jet decreases further, and thus the bubble diameter increases to some limit, the void profile changes from a saddle shape into a convex shape, with the sliding bubbles near the wall gathering into the center of the tube. Similar results were also reported by Serizawa *et al.* (1988).

After examining the entire results of the present study, the critical bubble diameter causing the above-mentioned void profile transfiguration is about 5–6 mm. The effects of bubble size on bubble development were observed by Sekoguchi *et al.* (1979) and Kariyasaki (1985) with a single bubble stream. They reported that bubbles of diameter <5 mm will move closer to the wall. Matsui (1988) indicated that bubbles of diameter >4 mm rise in the core region of the channel, based on his experimental result under an extremely low void ($\langle\epsilon\rangle = 1.7\%$) condition. A strong dependence of the phase distribution and bubble number frequency on the bubble size distribution in a concentrated bubbly flow regime was also found in this study with almost the same critical bubble diameter.

In general, the void profile transfiguration often occurred with bubble coalescence and bubble growth. As L/D increases to some extent, depending on the test-section liquid and gas flow rates, the flow regime transition from bubbly to slug flow may occur. Serizawa & Kataoka (1987) summarized the observed four major void distribution patterns (wall peak, intermediate peak, transition and core peak) in the flow regime map shown in figure 7. From the discussion above,

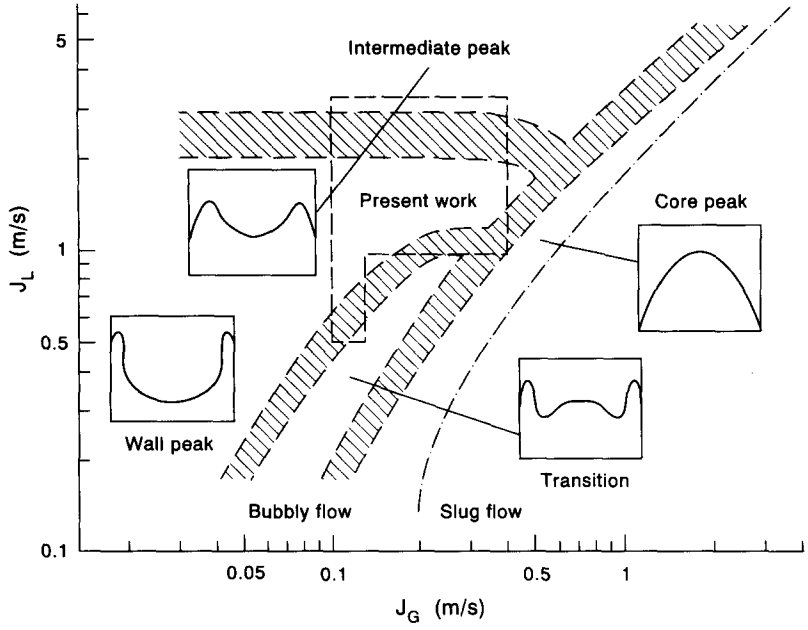

Figure 7. A simple model of the phase distribution pattern (Serizawa & Kataoka 1987).

it is clear that void distribution patterns may not be characterized completely by the volumetric fluxes of both phases. Indeed, by changing the bubble size, more than one phase distribution pattern may appear under the fixed volumetric flux combinations (J_L and J_G). This phenomena is especially significant under low liquid flow conditions. The experimental data of Serizawa *et al.* (1988) also support this conclusion.

4.4. Mean phases velocity effect on the void profile

The influence of the mean phases velocity on the void profile depends on the initial bubble diameter. Figures 8(a–c) present the (mean) liquid phase velocity effect on the void fraction, bubble size and bubble frequency distributions under the same gas phase velocity ($J_G = 0.1$ m/s) condition. The bubble size condition was changed by two different liquid jet velocities. From figure 8(b), it is interesting to note that in the low liquid jet velocity condition ($J_j = 1.0$ m/s, open symbols) the large bubbles tend to gather into the channel center at the two lower liquid velocities ($J_L = 0.5$ and 1.0 m/s), resulting in a parabolic bubble diameter profile. A further increase in the liquid velocity ($J_L = 2.0$ m/s) will decrease the bubble size and flatten the bubble diameter profile. Figure 8(c) shows that most of the bubbles for all these J_L are distributed uniformly across the channel, even though the number of small size bubbles is considerable in the high liquid velocity condition. Thus, the resultant void fraction distribution at low liquid flows shows a parabolic profile. In contrast, as the liquid flow increases a more uniform void distribution will result.

As the liquid jet increases to $J_j = 2.0$ m/s (solid symbols) under the same conditions as before, figure 8(b) shows that the bubble size decreased significantly under low liquid velocity conditions ($J_L = 0.5$ and 1.0 m/s), while the original small bubbles just decreased in slightly under the high liquid flow condition. Thus, the bubble size tends to distribute more uniformly across the channel for all three liquid flow conditions. Figure 8(c) shows the consistent tendency of bubble movement for most of these small bubbles to migrate towards the wall to form a peaking profile. By considering the tendency of the bubble size and bubble frequency profiles discussed above, it is clear that the effect of the liquid velocity on the void fraction profile is more sensitive under low liquid flow conditions. As the liquid jet velocity increases, the void fraction profile shows a drastic change from parabolic to wall peaking in the low liquid condition and a slight change in the high liquid condition.

Figures 9(a–c) present typical results of the gas phase velocity effect on the void fraction, bubble size and bubble frequency distribution under the same bulk liquid flow rate ($J_L = 2.0$ m/s) condition. The bubble size condition was also changed by two different liquid jet velocities. With

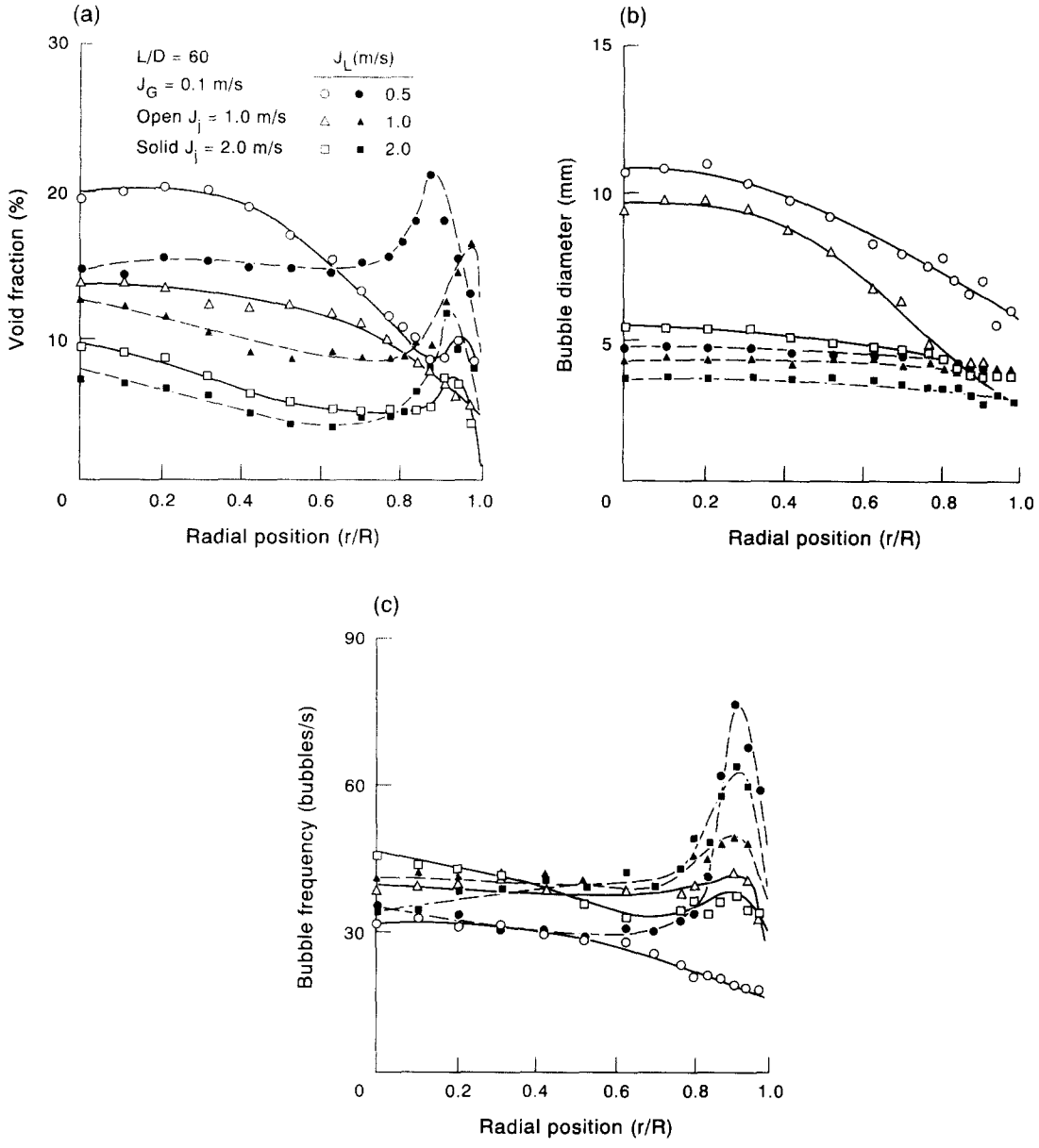

Figure 8. Liquid velocity effect on the (a) void fraction, (b) bubble size and (c) bubble frequency distributions.

a low velocity liquid jet ($J_j = 1.0$ m/s, open symbols), the profiles of bubble diameter and bubble frequency change from nearly uniform to parabolic as the gas velocity increases. Thus, the resulting void fraction radial profiles show the same tendency as those of the bubble diameter and bubble frequency. Furthermore, by increasing the jet velocity to a higher value ($J_j = 4.0$ m/s, solid symbols), the bubble size decreases drastically and bubbles are distributed more uniformly across the channel for the high J_G condition. Large numbers of these small bubbles tend to migrate toward the channel wall, resulting in a uniform bubble frequency distribution in the core region and a very sharp peak near the wall. Thus, the profile of void fraction will follow the same trend as the bubble frequency in changing from coring to wall peaking.

From the above results, it should be noted that higher mean liquid velocities lead to more uniform void profiles with wall peaking and a decreased effect of the nozzle jet speed (or bubble size) on the void fraction distribution. In contrast, the higher the mean gas velocity, the more parabolic will be the void profile, and thus the greater the influence of the nozzle jet speed on the void fraction distribution. The resultant void profile will strongly depend on the bubble size, bubble

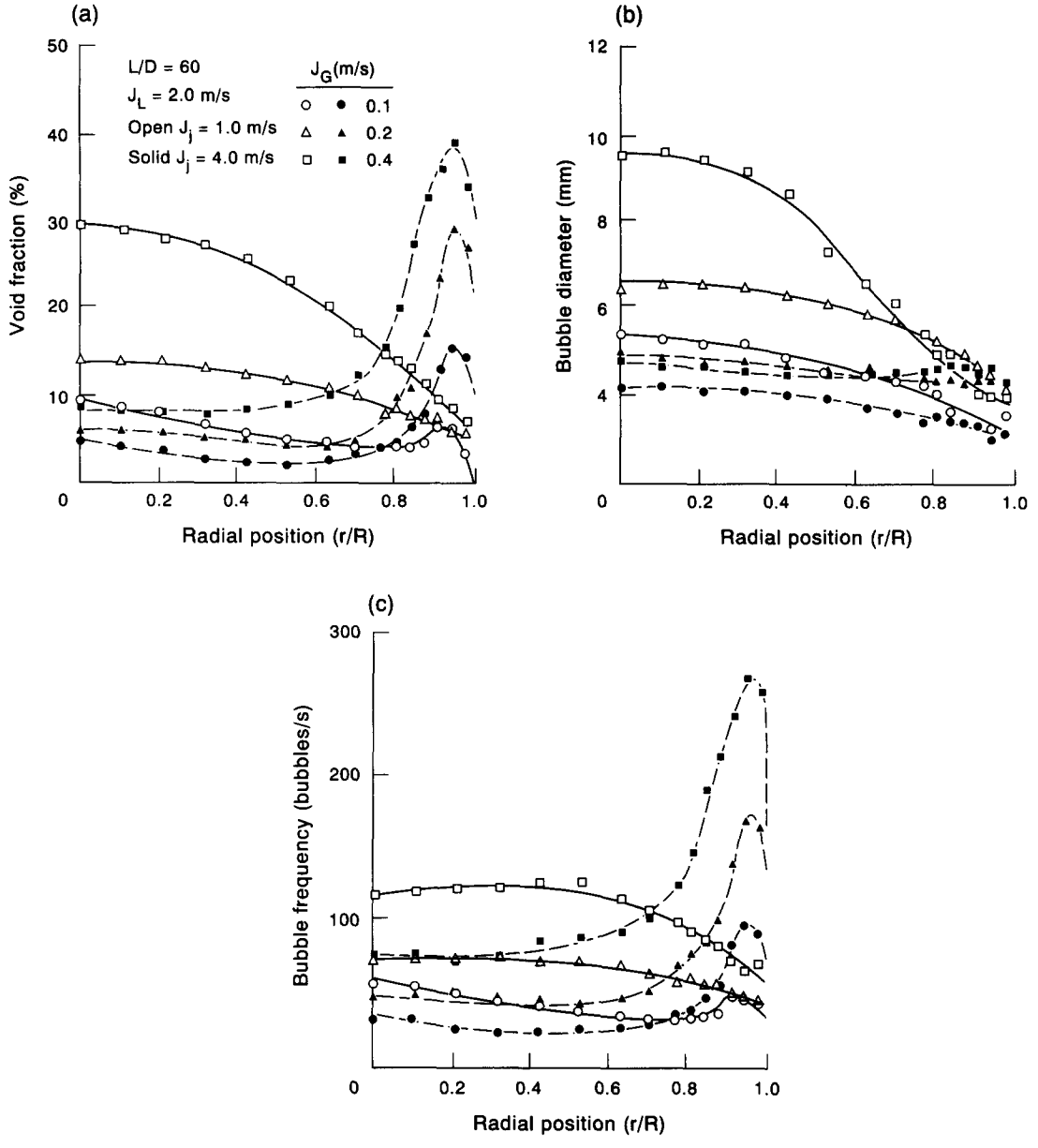

Figure 9. Gas velocity effect on the (a) void fraction, (b) bubble size and (c) bubble frequency distributions.

movement and mean velocity of both phases, which could be satisfactorily explained from the variation of bubble size, bubble frequency and their distributions. Thus, in considering the gas or liquid phase effect on the void distribution, the bubble size conditions also need to be specified clearly.

4.5. Entrance length effect

Figure 10(a) presents typical results of void fraction profiles at the fixed J_G and J_j under two liquid fluxes of $J_L = 1.0$ (open symbols) and 3.0 m/s (solid symbols), obtained at $L/D = 30$, 60, 90 and 120 respectively, from the outlet of the bubble injector. Due to the high liquid jet used to generate small bubbles, bubbly flow is formed throughout the channel. It is known from the former discussion about the flow regime development that the higher the liquid jet, the larger the axial length which can be sustained for small bubbles flowing through; thus a wall peaking void distribution can be maintained longer. However, at a fixed liquid jet velocity under $J_L = 1.0$ m/s, figure 10(a) indicates that with increasing entrance length, these peaks tend to decrease and finally may completely vanish. This could also be explained by the measured bubble size, frequency and

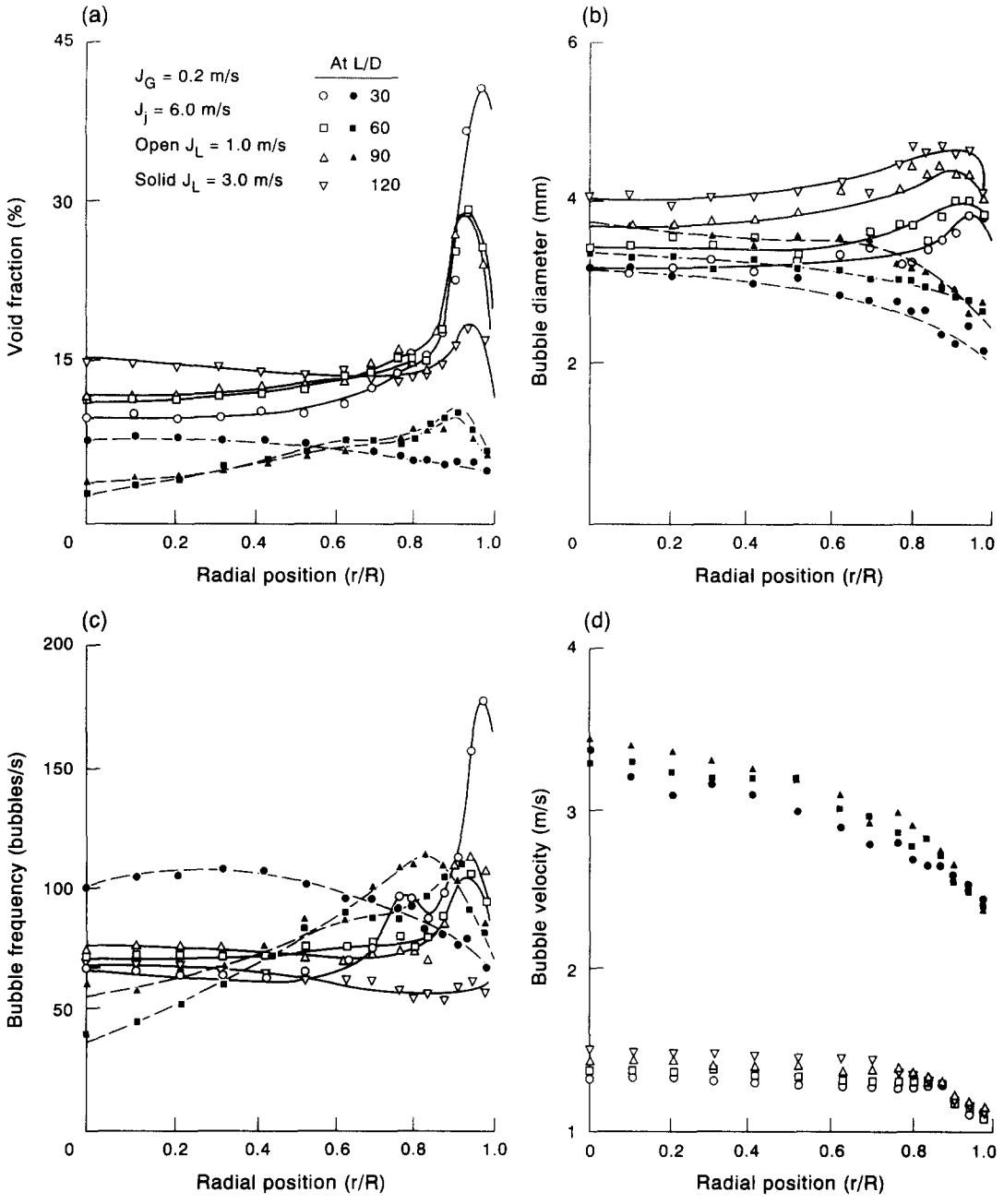

Figure 10. L/D effect on the (a) void fraction, (b) bubble size, (c) bubble frequency and (d) bubble velocity distributions.

velocity distributions, as shown in figures 10(b–d). From figure 10(b), the bubble size is nearly uniformly distributed in the cross-section area and increases slightly as L/D increases. However, from figure 10(c), the peaking bubble density near the wall tends to decrease as L/D increases and finally almost disappears at $L/D = 120$. This bubble number redistribution along the channel may be partially due to the higher collision rate between these highly concentrated bubbles near the channel wall, which increases the probability of bubble coalescence and the tendency to agglomerate, partially due to the large turbulent fluctuations, as well as due to the effects related to the velocity gradient, bubbles are then periodically transported into the channel core. As a result, the peak height of the void profile decreases with the distance from the injection point. Figure 10(d) presents typical development profiles of bubble velocity, which are characterized by a fair uniform distribution over a large portion of the flow area and with a slight increase as the bubble size

increases with the distance from the injection point. This is exactly the same tendency observed in the entrance region.

For the higher liquid flux condition, such as at $J_L = 3.0$ m/s, after $L/D = 30$, there are no significant differences in the development of the void fraction, bubble size and bubble frequency profiles along the length of the bubble flow channel. This result suggests that the decrease in sensitivity to the initial condition with increased distance from the inlet and the hydrodynamic equilibrium of vertical upward bubbly flow could be attained in a short distance from the entrance. This is in agreement with the results of Serizawa *et al.* (1975) and Avdeev (1984). The reason for this type of bubbly flow is due to a turbulent dispersion of bubbles by the mixing action of turbulent flow, which have sufficient energy to break large bubbles into small ones, thus keeping this small bubble in a fixed profile flowing along the channel. However, Takamasa (1989) reported that the void profile tends to develop towards a common power-law profile for $L/D > 150$, while Herringe & Davis (1976) reported a common wall peaking void profile at $L/D = 108$, independent of the inlet conditions, even though different profiles are formed during flow development. Recently, Hewitt (1990) also reported that there was no effect of channel length on the flow regime transition condition. The conclusion is based on the cross-sectional averaged void fraction data of liquid superficial velocities < 1.0 m/s, which showed no significant change with length when plotted against local gas superficial velocity. In this study, the detailed local measurements at $J_L > 1.0$ m/s under small bubble conditions generally support this conclusion. However, for bubbly flow under low liquid velocities (such as $J_L = 0.5$ m/s at small J_G), as discussed above, bubble coalescence occurs gradually along the channel, as well as a buoyancy effect, leading to larger bubbles and ultimately to bubbles which have a similar diameter to the pipe and hence to the slug flow observed in this study and by previous investigators, such as Taitel *et al.* (1980). The inconsistency may be due to the different bubble size as well as the bubble generating method.

5. SUMMARY AND CONCLUSIONS

The effects of bubble size and entrance length on the void distribution in a vertical upward cocurrent air–water two-phase flow have been studied systematically based on the measurement of a dual-sensor resistivity probe. Under the well-controlled initial bubble size flow conditions, profiles of void fraction, bubble frequency, bubble velocity and bubble size were measured simultaneously—covering a broad range of a total of 115 combinations of (J_L, J_G, J_j and L/D) conditions. In this paper, the various bubble size effects on the void distribution have been discussed based on the bubble diameter, bubble frequency and their distribution. The results indicate that the bubble lateral migration and flow regime transition are very sensitive to the variation in bubble size and the bubble coalescence effect during the development of bubbly flow. Both the bubble lateral migration and flow regime transition also showed a strong dependence on the liquid and gas volumetric fluxes. The important results are summarized as follows:

(1) The different bubble sizes in two-phase flow may change the flow regime even under the fixed gas and liquid volumetric fluxes and geometry condition. However, the existing published flow regime maps cannot reflect this result and could also be one of the reasons for the inconsistency between them.
(2) In bubbly flow, the lateral void distribution is found to be very sensitive to bubble size. Generally, the smaller the bubbles generated, the more uniform is the bubble size distributed across the channel. Most of these bubbles preferably migrate toward the wall. As the bubble size increases to some limit, the void profile changes from a saddle shape into a convex shape. The critical bubble diameter causing the void profile transfiguration is found to be 5–6 mm. Moreover, by changing the bubble size, more than one phase distribution pattern (such as wall peaking, intermediate peaking, transition and coring) may appear with fixed two-phase volumetric fluxes.
(3) The effect of bubble size on the lateral void fraction shows a strong dependence on the two-phase volumetric fluxes. The results indicate that higher mean liquid velocities lead to more uniform void profiles with wall peaking, and a

decreased effect of the nozzle jet speed (or bubble size) on the void fraction distribution. In contrast, the higher the mean gas velocity, the more parabolic will be the void profile, and thus the greater the influence of the nozzle jet speed on the void fraction distribution.

(4) The L/D effect is also a critical factor in the lateral void distribution. It closely relates the bubble coalescence in low liquid flow and the bubble break-up in high liquid flow. These two effects resulted in different bubble size and frequency; thus they are directly related to the phase distribution and flow regime transition.

(5) The attainability of hydrodynamic equilibrium [i.e. $F(r/R, L/D) = F(r/R)$] for the phase development along the channel also depends on the bubble size. For very low flow conditions (such as $J_L \leq 0.5$ m/s with $D_b \geq 5$ mm), the so-called fully developed condition of a parabolic void profile could be reached after $L/D = 100$. However, for the high liquid and low gas flow conditions (such as $J_L \geq 2.0$ m/s, $J_G \leq 0.2$ m/s with $D_b \leq 5$ mm), the same void profile with wall peaking will be maintained after $L/D = 60$.

From these results, one concludes that the bubble size is a key parameter in two-phase flow and is very sensitive to the void distribution and flow structure. Hence, existing models, which are to be valid over a wide range of conditions, should include the effect of bubble size.

Acknowledgements—The author wishes to express his gratitude to Mr F. Z. Yeh and Mr W. T. Hong, for their help in performing the experiments.

REFERENCES

AVDEEV, A. A. 1984 Turbulent flow hydraulics of bubbly two-phase mixture. *High Temp.* **21,** 536–544.

HERRINGE, R. A. & DAVIS, M. R. 1976 Structure development of gas–liquid mixture flows. *J. Fluid Mech.* **73,** 97–123.

HEWITT, G. F. 1990 Non-equilibrium two-phase flow. In *Proc. 9th Int. Heat Transfer Conf.*, Jerusalem, Israel, Vol. 1, pp. 383–394.

JONES, O. C. JR & ZUBER, N. 1978 Use of a cylindrical hot-film anemometer for measurement of two-phase void and volume flux profiles in a narrow rectangular channel. *AIChE Symp. Ser.* **74,** 191–204.

KARIYASAKI, A. 1985 Behaviour of a gas bubble in a liquid flow with a linear velocity profile. Presented at the *7th Two-Phase Flow Symp. of Japan.*

KATAOKA, I. & SERIZAWA, A. 1990 Interfacial area concentration in bubbly flow. *Nucl. Engng Des.* **120,** 163–180.

KOBAYASHI, T., IIDA, Y. & KANEGAE, N. 1970 Distribution of local void fraction of air–water two-phase flow in a vertical channel. *Bull. JSME* **13,** 1005–1012.

LACKME, C. 1967 Structure and kinematics of two-phase bubbly flow. CEA Report CEA-R 3203.

LAHEY, R. T. JR 1988 Turbulence and phase distribution phenomena. In *Proc. Transient Phenomena in Multiphase Flow—ICHMT Int. Semin.*, Dubrovnik, Croatia, pp. 139–177.

LAHEY, R. T. JR 1990 The analysis of phase separation and phase distribution phenomena using two-fluid models. *Nucl. Engng Des.* **122,** 17–40.

LIU, T. J. 1989 Experimental investigation of turbulence structure in two-phase bubbly flow. Ph.D. Thesis, Northwestern Univ., Evanston, IL.

LIU, T. J. 1990 Bubble size effect on phase distribution and turbulent structure I: air/water loop design and test plan. INER Report INER-T1407.

LIU, T. J. 1991 The effect of bubble size on void fraction distribution in a vertical channel. In *Proc. Int. Conf. on Multiphase Flows '91*, Tsukuba, Japan, pp. 453–457.

LIU, T. J. & BANKOFF, S. G. 1993 Structure of air–water bubbly flow in a vertical pipe: II—void fraction, bubble velocity and bubble size distribution. *Int. J. Heat Mass Transfer.* **36**(4). In press.

MATSUI, G. 1988 Characteristic structure of upward bubble flow under the same flow rate conditions. In *Proc. Japan–U.S. Semin. on Two-phase Flow Dynamics*, Ohtsu, Japan, pp. E.2-1–E.2-10.

MICHIYOSHI, I. & SERIZAWA, A. 1986 Turbulence in two-phase bubble flow. *Nucl. Engng Des.* **95,** 253–267.

ROUHANI, Z. 1976 Effect of wall friction and vortex generation on radial void distribution, the wall–vortex effect. *Int. J. Multiphase Flow* **3,** 35–50.

SEKOGUCHI, K., FUKUI, H. & SATO, Y. 1979 Flow characteristic and heat transfer in vertical bubble flow. Presented at the *Japan–U.S. Semin. on Two-phase Flow Dynamics*, Kansai, Japan.

SERIZAWA, A. & KATAOKA, I. 1987 Phase distribution in two-phase flow. In *Proc. Transient Phenomena in Multiphase Flow—ICHMT Int. Semin.*, Dubrovnik, Croatia, pp. 179–224.

SERIZAWA, A., KATAOKA, I. & MICHIYOSHI, I. 1975 Turbulence structure of air–water bubbly flow. *Int. J. Multiphase Flow* **2,** 221–246.

SERIZAWA, A., KATAOKA, I., ZUN I. & MICHIYOSHI, I. 1988 Bubble size effect on phase distribution. In *Proc. Japan–U.S. Semin. on Two-phase Flow Dynamics*, Ohtsu, Japan, pp. 15–20.

SERIZAWA, A., KATAOKA, I., GOFUKU, A., TAKAHASHI, O. & KAWARA, Z. 1991 Effect of initial bubble size on bubbly flow structure. In *Proc. Int. Conf. on Multiphase Flows '91*, Tsukuba, Japan, pp. 547–550.

SUBBOTIN, V. I. 1971 Turbulent channel flow characteristics of gas–water mixtures. *Sov. Phys. Dokl.* **16,** 192–194.

TAITEL, Y., BARNEA, D. & DUKLER, A. E. 1980 Modeling flow pattern transition for steady upward gas-liquid flow in vertical tubes. *AIChE Jl* **26,** 345–354.

TAKAMASA, T. 1989 Effect of wall roughness on developing vertical bubbly flow. In *Turbulence Modification in Dispersed Multiphase Flows*, Vol. 80, pp. 73–80. ASME, New York.

VAN DER WELLE, R. 1985 Void fraction bubble velocity and bubble size in two-phase flow. *Int. J. Multiphase Flow* **11,** 317–345.

WALLIS, G. B. & RICHTER, H. J. 1973 Influence of walls on bubble motion in vertical two-phase flow. Thayer School of Engineering, Dartmouth College, Hanover, NH.

WANG, S. K., LEE, S. J., JONES, O. C. JR & LAHEY, R. T. JR 1987 3-D Turbulence structure and phase distribution measurements in bubbly two-phase flow. *Int. J. Multiphase Flow* **13,** 327–340.

ZUN, I. 1980 The transverse migration of bubbles influenced by wall in a vertical bubbly flow. *Int. J. Multiphase Flow* **6,** 583–588.

ZUN, I. 1988 Transition from wall void peaking to core void peaking in turbulent bubbly flow. In *Proc. Transient Phenomena in Multiphase Flow—ICHMT Int. Semin.*, Dubrovnik, Croatia, pp. 225–245.